Plastic Cyclic Analysis Using Linear Yield Surface

By Morteza A. M. Torkamani,[1] M. ASCE and Mohammad R. Pajand[2]

Abstract: Tresca type yield surfaces suitable for a kinematic hardening formulation of incremental theory of plasticity are presented. A uniaxial symmetric Tresca yield condition, along with a linear kinematic hardening rule, is utilized to formulate a small displacement, plane stress incremental theory of plasticity. This theory is applicable to materials with both equal and unequal tension and compression yield stress. Constitutive laws for sides and corners of the yield surface are derived. Finite element formulation, numerical solution and application are discussed.

Introduction

Incremental theories of plasticity, along with the finite element direct stiffness method, have been used widely for inelastic structural analysis. A solution procedure for the elasto-plastic problem is to find the incremental displacements from the equilibrium equations and proceed to calculate incremental strains and stresses. The load may be applied to the structure in incremental form. At any step of the analysis, the total displacements, strains, and stresses can be found. A new stiffness matrix can be formed for any state of stress, and the analysis continued for the next step. During any step of the analysis, the state of stress must satisfy the yield criterion.

In the past, most of the elasto-plastic finite element formulations have used the von Mises yield condition. The primary reason for wide usage of the von Mises yield surface, besides the experimental justification for some materials, is the mathematical description of the surface. The von Mises yield surface is defined by one smooth elliptical curve, which is simpler than other yield conditions for the derivation of constitutive laws and computer coding. Among the many excellent studies that have used the von Mises yield condition, utilizing both initial strain and initial stress approaches, the following are prominent: Refs. 7, 8, 11, 13–15, 18, 21, and 23.

Experimental research by Phillips and others shows that the yield surface of metals lies between the von Mises and Tresca surfaces (12,10). Phillips also shows that the yield surface for many metals closely follows the Tresca surface (12). Anand and his colleagues used the Tresca yield condition and isotropic hardening, subject to only monotonically increasing loads, to formulate several plane stress and plane strain plasticity theories (2,3,4,5). However, theory involving the Tresca type yield condition and the kinematic hardening rule, which is suitable for cyclic

[1]Asst. Prof., Dept. of Civ. Engrg., Univ. of Pittsburgh, Pittsburgh, Pa. 15261.
[2]Former Grad. Student, Dept. of Civ. Engrg., Univ. of Pittsburgh, Pittsburgh, Pa. 15261.

Note.—Discussion open until October 1, 1984. To extend the closing date one month, a written request must be filed with the ASCE Manager of Technical and Professional Publications. The manuscript for this paper was submitted for review and possible publication on August 10, 1983. This paper is part of the *Journal of Engineering Mechanics*, Vol. 110, No. 5, May, 1984. ©ASCE, ISSN 0733-9399/84/0005-0776/$01.00. Paper No. 18783.

loading, should also be considered and is the subject of this paper.

The contribution of this work to the area of plasticity is threefold: (1) It uses a linear yield surface with vertices, together with a kinematic hardening rule, whose use might become advantageous in some cases in which materials do not retain a smooth yield surface after initial yield, especially for nonmonotonic loading cases; (2) the formulation is suitable for the elasto-plastic analysis of the plane stress problem under static and cyclic loading; and (3) the selected yield condition can be utilized for the approximate elasto-plastic analysis of tension-weak materials such as soil, concrete, glass, and ice.

In order to formulate the elasto-plastic analysis, the constitutive laws have to be established. Establishment of the constitutive laws requires three items: initial yield condition, hardening rule, and flow rule. In this study, the uniaxial symmetric Tresca yield surface was selected for the yield condition. The uniaxial symmetric Tresca yield surface is defined as a yield surface with unequal axial tensile and compressive yield stresses. It is symmetric about an axis passing through the origin and making an angle of 45 degrees with the σ_1 axis. In contrast, the more usual Tresca yield surface is a center symmetric yield surface. Ziegler's modification of Prager's kinematic hardening rule, which is suitable for loading and unloading and considers Bauschinger's effect, was chosen for establishing the conditions for subsequent yield from a plastic state (22). A comprehensive discussion of different kinematic hardening rules and justification for choosing the Ziegler's hardening rule is given in Ref. 6. The associated flow rule for the uniaxial symmetric Tresca yield condition, and the kinematic hardening for linear hardening material, were employed in order to relate the plastic strain increments to the stresses and stress increments.

Yield Condition

The general form of a yield condition suitable for kinematic hardening may be expressed as

$$F(\{\sigma - \alpha\}) = 0 \qquad (1)$$

in which $\{\sigma\}$ = the state of stresses; and $\{\alpha\}$ = a vector relating the spatial position of the yield surface to the plastic history of the material.

Tresca Yield Condition.—The center symmetric Tresca yield condition for the plane stress problem, in terms of principal stresses, may be expressed as

$$F(\{\bar{\sigma}\}) = [(\bar{\sigma}_1 - \bar{\sigma}_2)^2 - \sigma_o^2](\bar{\sigma}_1^2 - \sigma_o^2)(\bar{\sigma}_2^2 - \sigma_o^2) = 0 \qquad (2)$$

in which $\bar{\sigma}_i = \sigma_i - \alpha_i$; and α_o = twice the maximum permissible shearing stress in the elastic state in tension. Eq. 2 may be expanded to a set of six functions, each defining one face or side of the hexagonal yield surface.

The frequently used center symmetric Tresca yield condition does not represent the behavior of a material with different tensile and compressive yield strengths. In order to extend the generality of the constitutive relationships, and to formulate a plasticity theory applicable to a material with equal or unequal tensile and compressive yield strengths, the uniaxial symmetric Tresca yield condition is used in this paper (see Fig. 1).

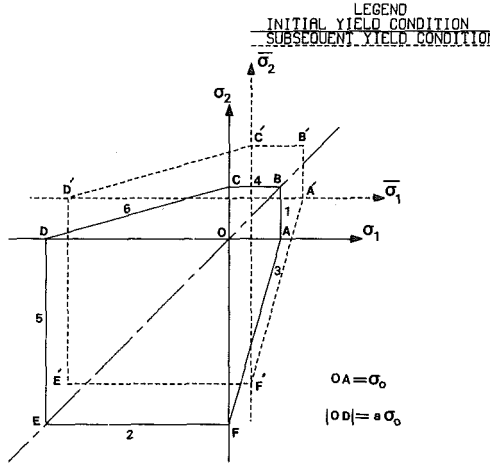

FIG. 1.—Uniaxial Symmetric Tresca Yield Condition

The equation of this yield surface, in terms of principal stresses, can be obtained by writing equations for all six sides of the hexagon as

$$F^1 = \bar{\sigma}_1 - \sigma_o = 0; \quad F^2 = -\bar{\sigma}_2 - a\sigma_o = 0; \quad F^3 = a\bar{\sigma}_1 - \bar{\sigma}_2 - a\sigma_o = 0;$$

$$F^4 = \bar{\sigma}_2 - \sigma_o = 0; \quad F^5 = -\bar{\sigma}_1 - a\sigma_o = 0; \quad F^6 = a\bar{\sigma}_2 - \bar{\sigma}_1 - a\sigma_o = 0 \quad \ldots \quad (3)$$

It is noted that the mathematical difference between the center symmetric and uniaxial symmetric yield conditions is expressed by the parameter a, in which $a = \sigma_c/\sigma_t$. σ_c and σ_t are the yield stresses in compression and tension, respectively. If $a = 1.0$, the yield condition will be center symmetric; otherwise, it is in the general form of the uniaxial symmetric Tresca yield condition.

By invoking the relationship between principal stresses and Cartesian stresses, these yield functions may be written as

$$F^1 = c^2\bar{\sigma}_x + s^2\bar{\sigma}_y + 2cs\bar{\sigma}_{xy} - \sigma_o = 0;$$

$$F^2 = -s^2\bar{\sigma}_x - c^2\bar{\sigma}_y + 2cs\bar{\sigma}_{xy} - a\sigma_o = 0;$$

$$F^3 = (ac^2 - s^2)\bar{\sigma}_x + (as^2 - c^2)\bar{\sigma}_y + 2cs(1 + a)\bar{\sigma}_{xy} - a\sigma_o = 0;$$

$$F^4 = s^2\bar{\sigma}_x + c^2\bar{\sigma}_y - 2cs\bar{\sigma}_{xy} - \sigma_o = 0;$$

$$F^5 = -c^2\bar{\sigma}_x - s^2\bar{\sigma}_y - 2cs\bar{\sigma}_{xy} - a\sigma_o = 0;$$

$$F^6 = (as^2 - c^2)\bar{\sigma}_x + (ac^2 - s^2)\bar{\sigma}_y - 2cs(1 + a)\bar{\sigma}_{xy} - a\sigma_o = 0 \quad \ldots\ldots\ldots\ldots \quad (4)$$

in which $c = \cos\theta$; $s = \sin\theta$; and θ = the angle between the x-axis and the direction of the major principal stress measured positive counterclockwise.

Elasto-Plastic Constitutive Relationship

The uniaxial symmetric Tresca yield surface has six sides and six sin-

gular corners. Fig. 1 shows the initial and subsequent states of this yield surface in the principal stress space. Any stress point, depending on the state of stress, can be either inside the yield locus, which is the elastic state, or at the yield surface, which is a plastic case. Stress points outside the yield locus are not defined, and their values are inadmissible. In the elastic state, the constitutive laws are well known and the elasticity relationships are applicable. In the plastic case, the stress points are located at the yield surface. Depending on the location of the stress state at the yield locus, different constitutive relationships must be applied. However, because of the symmetry of the yield locus, only half of the yield condition needs to be utilized in the analysis.

Elasto-Plastic Stress-Strain Matrix for Sides

The yield function for side i of the uniaxial symmetric Tresca yield surface is expressed by

$$F^i[\{\sigma - \alpha\}] = 0 \quad (5)$$

in which $\{\sigma\}$ = the state of stress; and $\{\alpha\}$ = the position of the yield surface origin with respect to the origin of the initial stress space. The total derivative of Eq. 5 leads to

$$\left\{\frac{\partial F^i}{\partial \sigma}\right\} = -\left\{\frac{\partial F^i}{\partial \alpha}\right\} \quad (6)$$

and $$\left\{\frac{\partial F^i}{\partial \sigma}\right\}^T \{\delta\sigma - \delta\alpha\} = 0 \quad (7)$$

The flow rule, or normality principle, is given by

$$\{\delta\epsilon^p\} = \lambda_i \left\{\frac{\partial F^i}{\partial \sigma}\right\} \quad (8)$$

in which λ_i = a constant coefficient to be determined later. Decomposition of the total strain into elastic and plastic components can be expressed as

$$\{\delta\epsilon\} = \{\delta\epsilon^e\} + \{\delta\epsilon^p\} \quad (9)$$

Derivation of an elasto-plastic matrix for any side i, $[D]^i_{ep}$, considering the Tresca yield condition and isotropic hardening rule, is presented in Ref. 3. A similar procedure is utilized herein to derive the relationship between the increments of stresses and strains (see Ref. 19 for details). The final result is

$$\{\delta\sigma\} = \left[[D]_e - [D]_e \left\{\frac{\partial F^i}{\partial \sigma}\right\} [M]_i^{-1} \left\{\frac{\partial F^i}{\partial \sigma}\right\}^T [D]_e\right] \{\delta\epsilon\} \quad (10)$$

in which $[D]_e$ = an elasticity matrix containing the appropriate elastic material properties; and

$$[M]_i = H\left\{\frac{\partial F^i}{\partial \sigma}\right\}^T \left\{\frac{\partial F^i}{\partial \sigma}\right\} + \left\{\frac{\partial F^i}{\partial \sigma}\right\}^T [D]_e \left\{\frac{\partial F^i}{\partial \sigma}\right\} \quad (11)$$

The kinematic hardening rules provide two more conditions. According to Ziegler's modification of Prager's rule, these conditions are expressed by

$$\{\delta\alpha\} = \{\sigma - \alpha\}d\mu \quad (12)$$

$$\left\{\frac{\partial F^i}{\partial \sigma}\right\}^T \{\delta\sigma - H\delta\epsilon^p\} = 0 \quad (13)$$

In the above equation, H = the hardening properties of the material; and $d\mu$ = a constant. The unknown constant, $d\mu$, can be evaluated by utilizing Eqs. 7 and 12.

$$d\mu = \frac{\left\{\frac{\partial F^i}{\partial \sigma}\right\}^T \{\delta\sigma\}}{\left\{\frac{\partial F^i}{\partial \sigma}\right\}^T \{\sigma - \alpha\}} \quad (14)$$

Using Eq. 8 along with Eq. 13 leads to

$$\lambda_i = \frac{\left\{\frac{\partial F^i}{\partial \sigma}\right\}^T \{\delta\sigma\}}{H\left\{\frac{\partial F^i}{\partial \sigma}\right\}^T \left\{\frac{\partial F^i}{\partial \sigma}\right\}} \quad (15)$$

Substituting λ_i from Eq. 15 into Eq. 8 will result in the incremental form of the plastic strain-stress relationship:

$$\{\delta\epsilon^p\} = \frac{\left\{\frac{\partial F^i}{\partial \sigma}\right\}\left\{\frac{\partial F^i}{\partial \sigma}\right\}^T \{\delta\sigma\}}{H\left\{\frac{\partial F^i}{\partial \sigma}\right\}^T \left\{\frac{\partial F^i}{\partial \sigma}\right\}} \quad (16)$$

The previous equation can be utilized to evaluate the hardening coefficient, H. This may be done by imposing the uniaxial stress-strain relationship upon Eq. 16.

Plastic Stress-Strain Relations for Sides

Taking the larger principal stress in the direction one, or algebraically $\bar{\sigma}_1 \geqq \bar{\sigma}_2$, the stress points always lie on or below the 45° diagonal EOB. Therefore, it is required that the constitutive laws be defined only for three sides and four corners of the yield surface, namely sides AB, EF, and AF, and corners A, B, E, and F (see Fig. 1).

Side 1 (AB).—For $i = 1$, substituting the value of the derivatives of F^1 with respect to various stress components from Eq. 4 into Eq. 11 and simplifying yields

$$[M]_1 = H_1(1 + 2c^2s^2) + \frac{E}{1 - \nu^2} \quad (17)$$

This value of $[M]_1$ and the derivatives of F^1 in Eq. 4 are substituted into Eq. 10 to yield the plastic stress-strain matrix for side 1 as

$$[D]^i_{ep} = \frac{E}{1-\nu^2}\left(\begin{bmatrix} 1 & \nu & 0 \\ \nu & 1 & 0 \\ 0 & 0 & \frac{1-\nu}{2} \end{bmatrix}\right.$$

$$\left. - \frac{E}{[M]_i(1-\nu^2)}\begin{bmatrix} d_{11} & d_{12} & d_{13} \\ & d_{22} & d_{23} \\ \text{SYM} & & d_{33} \end{bmatrix}\right) \quad \text{(18)}$$

for $i = 1$, in which

$$d_{11} = (c^2 + \nu s^2)^2; \quad d_{12} = (c^2 + \nu s^2)(\nu c^2 + s^2); \quad d_{13} = cs(c^2 + \nu s^2)(1-\nu);$$

$$d_{22} = (\nu c^2 + s^2)^2; \quad d_{23} = cs(\nu c^2 + s^2)(1-\nu); \quad d_{33} = [cs(1-\nu)]^2 \quad \text{(19)}$$

The elasto-plastic matrix, $[D]^1_{ep}$, is related to the hardening parameter, H, which must be determined. Following the same procedure which was used by Armen for the von Mises yield condition and kinematic hardening rule (6), Eq. 16 is utilized for three components of stresses, $(\sigma_x, \sigma_y, \sigma_{xy})$, one at a time. For each stress component, a corresponding hardening parameter was defined, i.e., $H_x = (\partial\sigma_x/\partial\epsilon^p_x)$; $H_y = (\partial\sigma_y/\partial\epsilon^p_y)$; and $H_{xy} = (\partial\sigma_{xy}/\partial\epsilon^p_{xy})$. Final evaluation of H_x, H_y, H_{xy}, assuming an average value for H, leads to

$$H_1 = \frac{H'}{3} \quad \text{(20)}$$

In the equation, H' = the slope of the uniaxial stress-strain curve developed from test data.

Side 2 (EF).—Proceeding in the same manner as described for Side 1, the value of $[M]_2$ is given as

$$[M]_2 = H_2(1 + 2c^2s^2) + \frac{E}{1-\nu^2} \quad \text{(21)}$$

and the stiffness matrix $[D]^2_{ep}$ by Eq. 18, for $i = 2$, in which

$$d_{11} = (s^2 + \nu c^2)^2; \quad d_{12} = (s^2 + \nu c^2)(\nu s^2 + c^2);$$

$$d_{13} = -cs(s^2 + \nu c^2)(1-\nu); \quad d_{22} = (\nu s^2 + c^2)^2;$$

$$d_{23} = -cs(\nu s^2 + c^2)(1-\nu); \quad d_{33} = [cs(1-\nu)]^2; \quad H_2 = \frac{H'}{3} \quad \text{(22)}$$

Side 3 (AF).—Derivatives of yield function F^3 from Eq. 4 are again used in Eq. 11, which leads to

$$[M]_3 = H_3[a^2(1 - 2c^2s^2) + 1 + 2c^2s^2$$

$$+ 8ac^2s^2] + (a^2 + 1 - 2a\nu)\left(\frac{E}{1-\nu}\right) \quad \text{(23)}$$

and which, in conjunction with Eq. 10, yields the plastic stress-strain matrix for Side 3 as Eq. 18, for $i = 3$, in which

$$d_{11} = [(ac^2 - s^2) + \nu(as^2 - c^2)]^2;$$

$$d_{12} = [(ac^2 - s^2) + \nu(as^2 - c^2)][\nu(ac^2 - s^2) + (as^2 - c^2)];$$

$$d_{13} = [(ac^2 - s^2) + \nu(as^2 - c^2)](cs)(1 + a)(1 - \nu);$$

$$d_{22} = [\nu(ac^2 - s^2) + (as^2 - c^2)]^2;$$

$$d_{23} = [\nu(ac^2 - s^2) + (as^2 - c^2)](cs)(1 + a)(1 - \nu);$$

$$d_{33} = [cs(1 + a)(1 - \nu)]^2; \quad H_3 = \frac{H'}{3} \qquad (24)$$

Elasto-Plastic Stress-Strain Matrix for Corners

The yield function for any corner, i.e., corner j, consists of the yield functions for the adjacent sides, n and m. These functions and their total derivatives can be expressed as

$$F^n[\{\sigma - \alpha\}] = 0 \qquad (25)$$

$$F^m[\{\sigma - \alpha\}] = 0 \qquad (26)$$

$$\left\{\frac{\partial F^n}{\partial \sigma}\right\}^T \{\delta\sigma - \delta\alpha\} = 0 \qquad (27)$$

$$\left\{\frac{\partial F^m}{\partial \sigma}\right\}^T \{\delta\sigma - \delta\alpha\} = 0 \qquad (28)$$

Defining $$\left[\frac{\partial F^j}{\partial \sigma}\right] = \left[\left\{\frac{\partial F^n}{\partial \sigma}\right\} \middle| \left\{\frac{\partial F^m}{\partial \sigma}\right\}\right] \qquad (29)$$

Eqs. 27 and 28 can be transformed into the following relationships:

$$\left[\frac{\partial F^j}{\partial \sigma}\right]^T \{\delta\sigma - \delta\alpha\} = 0 \qquad (30)$$

$$\left[\frac{\partial F^j}{\partial \sigma}\right]^T \{\delta\sigma\} = \left[\frac{\partial F^j}{\partial \sigma}\right]^T \{\delta\alpha\} \qquad (31)$$

According to Koiter's generalization of the flow rule (9), the flow rule for corner j is given by

$$\{\delta\epsilon^p\} = \lambda^n \left\{\frac{\partial F^n}{\partial \sigma}\right\} + \lambda^m \left\{\frac{\partial F^m}{\partial \sigma}\right\} = \left[\frac{\partial F^j}{\partial \sigma}\right]\{\lambda^j\} \qquad (32)$$

with the specification that

$$\{\lambda^j\}^T = [\lambda^n \lambda^m] \qquad (33)$$

Decomposition of the total strain is given by Eq. 9.

A procedure similar to that used for the derivation of the elasto-plastic matrix for the sides is utilized to derive the elasto-plastic matrix for any corner j, $[D]^j_{ep}$. Ref. 19 presents the details of this derivation. The final

result is

$$\{\delta\sigma\} = \left[[D]_e = [D]_e \left[\frac{\partial F^j}{\partial \sigma}\right] [M^j]^{-1} \left[\frac{\partial F^j}{\partial \sigma}\right]^T [D]_e \right] \{\delta\epsilon\} \quad (34)$$

in which $$[M^j] = H\left[\frac{\partial F^j}{\partial \sigma}\right]^T \left[\frac{\partial F^j}{\partial \sigma}\right] + \left[\frac{\partial F^j}{\partial \sigma}\right]^T [D]_e \left[\frac{\partial F^j}{\partial \sigma}\right] \quad (35)$$

The kinematic hardening rule can be expressed as

$$\{\delta\alpha\} = \{\sigma - \alpha\} d\mu \quad (36)$$

$$\left[\frac{\partial F^j}{\partial \sigma}\right]^T \{\delta\sigma - H\delta\epsilon^p\} = 0 \quad (37)$$

Insertion of Eq. 36 into Eq. 31 leads to

$$\left[\frac{\partial F^j}{\partial \sigma}\right]^T \{\sigma - \alpha\} d\mu = \left[\frac{\partial F^j}{\partial \sigma}\right]^T \{\delta\sigma\} \quad (38)$$

Premultiplying Eq. 38 by $\{\delta\sigma\}^T[\partial F^j/\partial\sigma]$ and solving for $d\mu$ we obtain

$$d\mu = \frac{\{\delta\sigma\}^T \left[\frac{\partial F^j}{\partial \sigma}\right] \left[\frac{\partial F^j}{\partial \sigma}\right]^T \{\delta\sigma\}}{\{\delta\sigma\}^T \left[\frac{\partial F^j}{\partial \sigma}\right] \left[\frac{\partial F^j}{\partial \sigma}\right]^T \{\sigma - \alpha\}} \quad (39)$$

Insertion of Eq. 32 into Eq. 37 and premultiplication of the result by $[[\partial F^j/\partial\sigma]^T[\partial F^j/\partial\sigma]]^{-1}$ leads to

$$\{\lambda^j\} = \frac{1}{H}\left[\left[\frac{\partial F^j}{\partial \sigma}\right]^T \left[\frac{\partial F^j}{\partial \sigma}\right]\right]^{-1} \left[\frac{\partial F^j}{\partial \sigma}\right]^T \{\delta\sigma\} \quad (40)$$

Finally, substituting for $\{\lambda^j\}$ from Eq. 40 into Eq. 32 leads to the incremental plastic strain-stress relationship as

$$\{\delta\epsilon^p\} = \frac{1}{H}\left[\frac{\partial F^j}{\partial \sigma}\right]\left[\left[\frac{\partial F^j}{\partial \sigma}\right]^T \left[\frac{\partial F^j}{\partial \sigma}\right]\right]^{-1} \left[\frac{\partial F^j}{\partial \sigma}\right]^T \{\delta\sigma\} \quad (41)$$

Plastic Stress-Strain Relation for Corners

Corner A.—The value of matrix $[M^A]$ may be evaluated using Eq. 35 and derivatives of F^1 and F^3 from Eq. 4. Defining

$$[N^A] = [M^A]^{-1} = \begin{bmatrix} n_{11}^A & n_{12}^A \\ n_{21}^A & n_{22}^A \end{bmatrix} \quad (42)$$

the determinant of matrix $[M^A]$ and elements of matrix $[N^A]$ are presented as

$$\text{Det}\,[M^A] = \left[H(1 + 2c^2s^2) + \frac{E}{1 - \nu^2}\right]\Big\{H[(1 + 2c^2s^2)(1 + a^2) + 4ac^2s^2]$$

$$+\frac{E}{1-\nu^2}(a^2+1-2a\nu)\Bigg\} - \left\{H[a(1+2c^2s^2)+2c^2s^2]+\frac{E}{1-\nu^2}(a-\nu)\right\}^2;$$

$$n_{11}^A = \left(\frac{1}{\mathrm{Det}[M^A]}\right)\Bigg\{H[(1+2c^2s^2)(1+a^2)+4ac^2s^2]+\frac{E}{1-\nu^2}(a^2+1$$

$$-2a\nu)\Bigg\}; \quad n_{12}^A = n_{21}^A = \left(\frac{1}{\mathrm{Det}[M^A]}\right)\Bigg\{H[a(1+2c^2s^2)+2c^2s^2]$$

$$+\frac{E}{1-\nu^2}(a-\nu)\Bigg\}; \quad n_{22}^A = \left(\frac{1}{\mathrm{Det}[M^A]}\right)\left\{H(1+2c^2s^2)+\frac{E}{1-\nu^2}\right\} \ldots\ldots \quad (43)$$

Substitution of the value of $[D]_e$ and derivatives of F^1 and F^3 from Eq. 4 and matrix $[N^A]$ from Eq. 43 into Eq. 34 leads to the plastic stress-strain matrix for corner A as

$$[D]_{ep}^j = \frac{E}{1-\nu^2}\left(\begin{bmatrix} 1 & \nu & 0 \\ \nu & 1 & 0 \\ 0 & 0 & \frac{1-\nu}{2} \end{bmatrix} - \frac{E}{1-\nu^2}\begin{bmatrix} d_{11} & & d_{12} & & d_{13} \\ & & d_{22} & & d_{23} \\ & \mathrm{SYM} & & & d_{33} \end{bmatrix}\right) \ldots \quad (44)$$

for $j = A$, in which

$$d_{11} = n_{11}^A(A1)^2 - 2n_{12}^A(A1)(A2+\nu A3) + n_{22}^A(A2+\nu A3)^2;$$

$$d_{12} = n_{11}^A(A1)(A4) - n_{12}^A(A1)(\nu A2+A3) - n_{12}^A(A4)(A2+\nu A3)$$

$$+ n_{22}^A(A2+\nu A3)(\nu A2+A3); \quad d_{13} = cs(1-\nu)\{n_{11}^A(A1) - n_{12}^A(A2+\nu A3)$$

$$+ (1+a)[n_{12}^A(A1) - n_{22}^A(A2+\nu A3)]\}; \quad d_{22} = n_{11}^A(A4)^2 - 2n_{12}^A(A4)(\nu A2$$

$$+ A3) + n_{22}^A(\nu A2+A3)^2; \quad d_{23} = cs(1-\nu)\{n_{11}^A(A4) - n_{12}^A(\nu A2+A3)$$

$$+ (1+a)[n_{12}^A(A4) - n_{22}^A(\nu A2+A3)]\};$$

$$d_{33} = [cs(1-\nu)]^2[n_{11}^A + 2n_{12}^A(1+a) + n_{22}^A(1+a)^2];$$

$$A1 = c^2+\nu s^2; \quad A2 = s^2 - ac^2; \quad A3 = c^2 - as^2; \quad A4 = \nu c^2 + s^2 \ldots. \quad (45)$$

The parameter, H, for corner, A, can be obtained from Eq. 41. The procedure is to find H_x, H_y and H_{xy} corresponding to $(\partial\sigma_x/\partial\epsilon_x^p)$, $(\partial\sigma_y/\partial\epsilon_y^p)$ and $\partial\sigma_{xy}/\partial\epsilon_{xy}^p)$, respectively. Assuming an average value for H, one obtains the result $H = 2H'/3$.

Following the procedure previously outlined, stress-strain relations for corners B, E, and F may be derived. They are given as follows.

Corners B and E.—Stress-strain relations for these two corners are the same. Defining

$$[N^B] = [M^B]^{-1} = \begin{bmatrix} n_{11}^B & n_{12}^B \\ n_{21}^B & n_{22}^B \end{bmatrix} \ldots\ldots\ldots\ldots\ldots\ldots\ldots\ldots\ldots\ldots \quad (46)$$

elements of matrix $[N^B]$ are

$$n_{11}^B = n_{22}^B = \frac{H(1 + 2c^2s^2) + \dfrac{E}{1 - \nu^2}}{H^2(1 + 4c^2s^2) + \dfrac{E}{1 - \nu^2}(E + 2H) + \left(\dfrac{4HEc^2s^2}{1 - \nu}\right)};$$

$$n_{12}^B = n_{21}^B = \frac{2Hc^2s^2 - \dfrac{\nu E}{1 - \nu^2}}{H^2(1 + 4c^2s^2) + \dfrac{E}{1 - \nu^2}(E + 2H) + \left(\dfrac{4HEc^2s^2}{1 - \nu}\right)} \quad \text{(47)}$$

The elasto-plastic matrix for corner B is given by Eq. 44, for $j = B$, in which

$$d_{11} = n_{11}^B[(s^2 + \nu c^2)^2 + (c^2 + \nu s^2)^2] + 2n_{12}^B(c^2 + \nu s^2)(\nu c^2 + s^2);$$

$$d_{12} = 2n_{11}^B(c^2 + \nu s^2)(\nu c^2 + s^2) + n_{12}^B[(c^2 + \nu s^2)^2 + (\nu c^2 + s^2)^2];$$

$$d_{13} = cs(1 - \nu)^2(c^2 - s^2)(n_{11}^B - n_{12}^B);$$

$$d_{22} = n_{11}^B[(c^2 + \nu s^2)^2 + (\nu c^2 + s^2)^2] + 2n_{12}^B(c^2 + \nu s^2)(\nu c^2 + s^2);$$

$$d_{23} = cs(1 - \nu)^2(s^2 - c^2)(n_{11}^B - n_{12}^B);$$

$$d_{33} = 2[cs(1 - \nu)^2(n_{11}^B - n_{12}^B); \quad H' = \frac{2H'}{3} \quad \text{(48)}$$

Corner F.—Defining

$$[N^F] = [M^F]^{-1} = \begin{bmatrix} n_{11}^F & n_{12}^F \\ n_{21}^F & n_{22}^F \end{bmatrix} \quad \text{(49)}$$

the determinant of matrix $[M^F]$ and elements of matrix $[N^F]$ are presented as

$$\text{Det}\,[M^F] = (AF)H^2 + (BF)H + (CF);$$

$$AF = [(1 + 2c^2s^2)(1 + a^2) + 4c^2s^2](1 + 2c^2s^2) - (1 + 2ac^2s^2 + 2c^2s^2)^2\};$$

$$BF = \frac{E}{1 - \nu^2}\{[(1 + 2c^2s^2)(1 + a^2) + 4c^2s^2]$$

$$+ (1 + a^2 - 2a)(1 + 2c^2s^2) - 2(1 + 2ac^2s^2 + 2c^2s^2)(1 - a\nu)\};$$

$$CF = \frac{(aE)^2}{1 - \nu^2}; \quad n_{11}^F = \left(\frac{1}{\text{Det}[M^F]}\right)\left\{H(1 + 2c^2s^2) + \frac{E}{1 - \nu^2}\right\};$$

$$n_{12}^F = n_{21}^F = -\left(\frac{1}{\text{Det}[M^F]}\right)\left\{H(1 + 2ac^2s^2 + 2c^2s^2) + \frac{E}{1 - \nu^2}(1 - a\nu)\right\};$$

$$n_{22}^F = \left(\frac{1}{\text{Det}[M^F]}\right)\left\{H(1 + 2c^2s^2)(1 + a^2) + 4c^2s^2\right]$$

$$+ \frac{E}{1 - \nu^2}(1 + a^2 - 2a\nu)\right\} \quad \text{(50)}$$

The elasto-plastic matrix for corner F is given by Eq. 44, for $j = F$, in which

$$d_{11} = n_{11}^F(F2 + \nu F3)^2 + 2n_{12}^F(F4)(F2 + \nu F3) + n_{22}^F(F4)^2;$$

$$d_{12} = n_{11}^F(F2 + \nu F3)(\nu F2 + F3) + n_{12}^F[(F5)(F2 + \nu F3) + (F4)(\nu F2 + F3)] + n_{22}^F(F4)(F5); \quad d_{13} = cs(\nu - 1)[n_{11}^F(F2 + \nu F3)(1 + a) + n_{12}^F(F2 + \nu F3 + F4 + aF4) + n_{22}^F(F4)]; \quad d_{22} = n_{11}^F(\nu F2 + F3)^2 + 2n_{12}^F(F5)(\nu F2 + F3) + n_{22}^F(F5)^2; \quad d_{23} = cs(\nu - 1)[n_{11}^F(\nu F2 + F3)(1 + a) + n_{12}^F(\nu F2 + F3 + F5 + aF5) + n_{22}^F(F5)];$$

$$d_{33} = [cs(1 - \nu)]^2[n_{11}^F(1 + a)^2 + 2n_{12}^F(1 + a) + n_{22}^F]; \quad H = \frac{2H'}{3};$$

$$F2 = s^2 - ac^2; \quad F3 = c^2 - as^2; \quad F4 = s^2 + \nu c^2; \quad F5 = c^2 + \nu s^2 \ldots\ldots \quad (51)$$

Finite Element Formulation

The constant strain triangular element (CST) is used in this study. The finite element formulation of the incremental equations of equilibrium, relating the nodal incremental displacements to incremental forces through the elasto-plastic stiffness matrix, is described in Refs. 5 and 19. The incremental force-displacement relationship of the whole structure in a global coordinate system is in the form

$$\{\delta Q\} = [K]_{ep}\{\delta q\} \ldots\ldots\ldots\ldots\ldots\ldots\ldots\ldots\ldots\ldots\ldots\ldots \quad (52)$$

in which $\{\delta Q\}$ = a column matrix of the incremental nodal forces; $\{\delta q\}$ = a column matrix of the incremental nodal displacements; and $[K]_{ep}$ = the stiffness matrix of the structure.

Solution Procedure

Among the many solution procedures for nonlinear static problems, a method of solution should be selected that is suitable for cyclic analysis, easy to implement, has the desired accuracy, and is computationally economical (17). Based on these factors, a combination of the tangent modulus and the residual force method was selected for the computational process (23).

For any step of the analysis, locating the stress point with respect to the yield surface will result in an elastic, plastic, or inadmissible state of stress. In the elastic or plastic case, the corresponding element stiffness can be utilized. For the stress points outside the yield surface, an inadmissible state, the stress point will be forced to the yield surface and the inadmissible part of the stresses will be calculated.

Solving equation $[K]_{ep}\{\delta q\} = \{\delta Q\}$, the incremental displacements can be found; then incremental strains and incremental stresses can be obtained. Adding these incremental values to the corresponding previously known values, the total displacements, strains, and stresses can be calculated at any stage of the process.

Although the solution obtained by this technique is in equilibrium at

any step, some stresses may violate the yield condition unless special corrective schemes are imposed during each load increment. If the total stresses are inadmissible stresses and exceed the yield surface by the amount of $\{\delta\sigma\}_c$, then these excess stresses can be assumed as initial stresses. These initial stresses exist within elements and are to be balanced by a set of nodal corrective forces, $\{P\}_c$. These nodal forces are expressed in the finite element formulation as

$$\{P\}_c = \int_{\mathrm{VOL}} [B]^T \{\delta\sigma\}_c dv \qquad (53)$$

Having the elastic properties of the element and the corrective nodal forces, $\{P\}_c$, incremental stresses are found, which can be corrected in a similar fashion, if necessary. The correction procedure is repeated until the stresses in all elements satisfy the yield condition and the corrective nodal forces, $\{P\}_c$, approach sufficiently small values. At this stage of analysis, equilibrium, as well as the yield criterion, is satisfied.

In the same way, the incremental value of the translation vector, which shifts the yield surface position, is obtained at any step. Superimposing this value on the stored value of the last step, the total value of the translation vector and, therefore, the position of the yield surface for the next step, will be known.

The remainder of the residual nodal forces, along with the next step incremental load, is applied to the structure at the beginning of each successive step. The same procedure is repeated for the next step, by updating the stiffness and finding the new displacements and stresses.

Loading and unloading criteria for sides and corners are well established. A summary of these conditions is presented in Ref. 19.

Examples

Two examples are presented herein. The purpose of the first example is to study the load-deflection behavior of a material, with unequal tension and compression yield strengths, under cyclic loading using elastoplastic analysis with a linear kinematic hardening rule and the Tresca yield surface.

A fixed-fixed end beam with rectangular cross section under a gradually and uniformly distributed cyclic load is considered for the first example. The beam is assumed to be made of material with linear elastic and perfect plastic behavior. The initial yield strength in tension is assumed to be 350.00 psi (2.41 MPa), and the corresponding value in compression is 10 times higher, 3,500.00 psi (24.13 MPa). The modulus of elasticity is assumed to be 3,500,000.00 psi (24,132.50 MPa), and Poisson's ratio is taken to be 0.15.

A graphical representation of the beam and finite element mesh is given in Fig. 2. In this figure, L = 72.00 in. (1,828.80 mm) and H = 12.00 in. (304.80 mm); the thickness of the beam is assumed to be 3.00 in. (76.20 mm).

The applied load is sinusoidal in the form of $F(t) = A \sin(\omega t)$, in which A = 750.00 lb/in. (131.34 N/mm) and ω = 1.0 rad/sec. Here t = a parameter to control the cyclic behavior of the load.

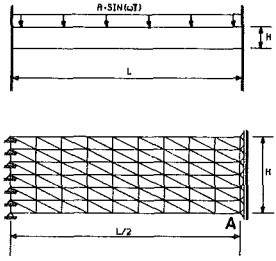

FIG. 2.—Mesh of Beam

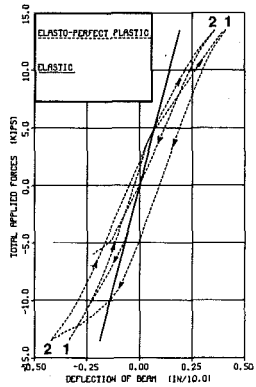

FIG. 3.—Two Cycle Load versus Displacement of Node at Center and Bottom of Beam

The load is applied incrementally, with a starting parameter increment of $\Delta t = 0.02$ sec. Since the applied load should be small in the plastic analysis, this parameter increment was reduced once the plastic region started and progressed. A total of 950 increments, equivalent to a parameter value of 13.024 sec, is considered in this case. This is more than two cycles of loading.

Due to the low tensile yield stress of the material, the first elements that yielded were those located at the top surface of the beam at the fixed supports. Progression of plastic enclaves continued at the supports toward the center of the beam, until the number of yielded elements at each support reached two. At this point, another plastic region started at the bottom and center of the beam. By increasing the applied load, the progression of plastic enclaves continued vertically at the supports and both horizontally and vertically at the center of the beam. When loading started in the opposite direction, another region of plasticity started at the bottom of the beam at the fixed supports.

The load-deflection relationship for point A, located at the center and bottom of the beam (see Fig. 2) is shown in Fig. 3. The horizontal shift of the hysteresis loops, with no vertical shifting, is an indication of elastic-perfectly plastic material behavior.

For the sake of comparison, a load-deflection curve of the same beam, considering elastic behavior and the same applied load, for a duration of 20.0 sec and the equivalent of 1,000 load increments, is shown in Fig. 3.

The purpose of the second example, which is a notched specimen, is threefold: (1) To compare the initial yield load of this example with that of the isotropic hardening rule to confirm the accuracy of the theory and computer program developed in this study; (2) to compare the progression of the plastic enclaves in the isotropic and kinematic hardening rules materials; and (3) to compare the distribution of the strains in the X and Y directions with the results of experimental research.

This example was previously investigated experimentally by Theocaris and Marketos (16), solved numerically by Allen and Southwell (1), and

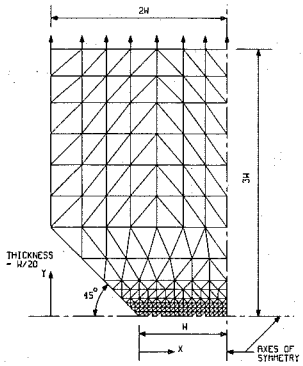

FIG. 4.—Mesh for Notched Specimen

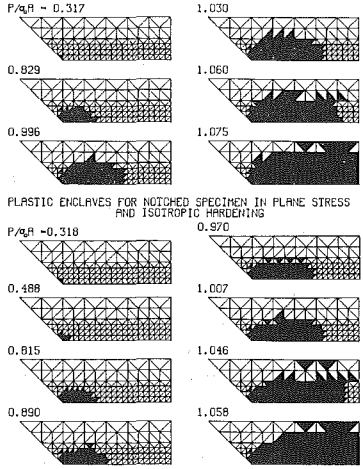

FIG. 5.—Plastic Enclaves for Notched Specimen in Plane Stress and Isotropic Hardening

solved by finite element analysis, assuming the von Mises yield condition, by Marcall and King (11), Yamada et al. (21), and Zienkiewicz et al. (23). Anand et al. (2) and Weisgerber (20) used the finite element method together with the Tresca yield condition for a perfectly plastic and isotropic hardening rule material in plane stress to obtain the stress and strain distribution in the notched specimen. Some of the results in these references are included for comparison purposes.

Fig. 4 shows the finite element mesh of 1/4 of the notched specimen, which is used in this paper. This mesh has 321 elements and 189 nodes and is as close as possible to that previously used by Anand and Weisgerber (3). The linear strain-hardening material has the following properties: the initial yield strengths in tension and compression are equal to 36.00 ksi (248.21 MPa); the modulus of elasticity is 30,000.00 ksi (206.84 GPa); and $H' = 0.032E$. A value of 0.30 is taken for Poisson's ratio. The applied load is taken in the form, $F(t) = A \sin(\omega t)$, with $A = 19.04$ kips/in. (3,334.26 N/mm) and $\omega = 1.00$ rad/sec.

The kinematic hardening formulation, presented in this paper, leads to the initial yield load of $P/A\sigma_0 = 0.318$, which is very close to the one reported by Anand and Weisgerber (3). Since the elastic solution is independent of the strain-hardening phenomenon, the difference is due to several factors, such as possible difference in finite element mesh points, the magnitude of the applied load increments, numerical solution differences, and others. It should be noted that two different magnitudes of loading have been considered for this example: (1) Cyclic loading—in this case unloading was started before plastic failure (the results of the cyclic loading are not reported here); and (2) monotonically increasing load up to plastic failure, for comparison with the isotropic hardening rule. However, once plastic flow has been initiated in the speci-

men, the progression of plastic enclaves is significantly affected by the hardening rule. Fig. 5 shows a comparison between the kinematic and isotropic hardening results. It is seen that the plastic region for the kinematic strain-hardening progresses faster across the plate than for the isotropic strain-hardening material. Therefore, the kinematic hardening plate has smaller plastic load carrying capacity than the isotropic strain-hardening one. Nevertheless, in both cases the plastic enclaves do tend to progress, basically, in the horizontal direction from the notch root when the Tresca yield condition is used.

The average strain distribution of the nodes along the minimum section of the specimen, expressed in terms of the initial yield strain, both in X and Y directions, is shown in Fig. 6. The strain distribution at $Y = 0.0$ is very close to that reported by Anand and Weisgerber (3), and the distribution pattern is similar to the experimental results of Theocaris and Marketos (16), except near the notch root. As mentioned by Weisgerber, this is attributed to the fact that the experimental specimen does have a small notch root radius, whereas the radius at the notch root of

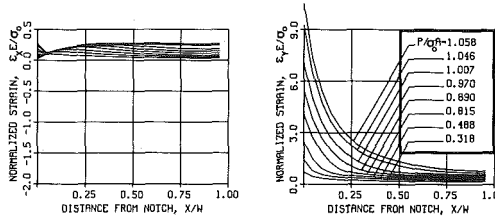

FIG. 6.—Average Strains of Nodes at $Y = 0.0$ for Notched Specimen in Plane Stress and Kinematic Hardening

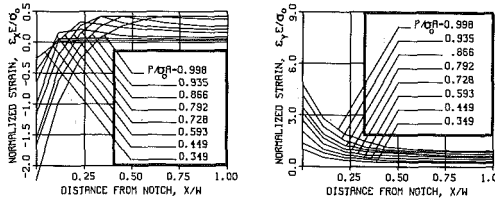

FIG. 7.—Strains from Experiment by Theocaris and Marketos

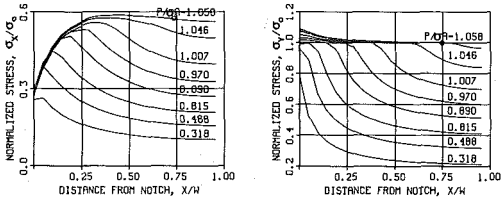

FIG. 8.—Average Stresses of Nodes at $Y = 0.0$ for Notched Specimen in Plane Stress and Kinematic Hardening

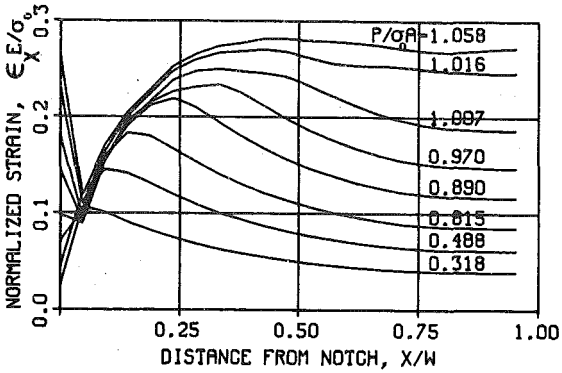

FIG. 9.—Average $E\epsilon_x/\sigma_o$ of Nodes at $Y = 0.0$ for Notched Specimen in Plane Stress and Kinematic Hardening

the specimen investigated by finite element analysis is zero. For the sake of clarification, $E\epsilon_x/\sigma_0$ obtained from the finite element results of Fig. 6 is expanded and is shown in Fig. 9. The strains obtained experimentally by Theocaris and Marketos are shown in Fig. 7.

The average stress distribution of the nodes along the minimum section of the specimen is shown in Fig. 8. The distribution of stresses σ_x/σ_0 at $Y = 0.0$ is again very close to the results reported in Ref. 3. The effect of the strain hardening property of the material in the Y-direction, i.e., on σ_y/σ_0, is clearly shown in this figure.

Conclusions

A formulation based on the incremental theory of plasticity with the assumption of small displacements was presented for the plane stress problem. This formulation uses kinematic hardening and the associated flow rule of the uniaxial symmetric Tresca yield function.

The constitutive equations were developed for the uniaxial symmetric Tresca yield surface. From these laws, the elasto-plastic matrices for the sides and corners of the yield locus were evaluated. These matrices were utilized in the elasto-plastic finite element analysis.

Through two examples, the procedure demonstrates the ability to trace the elasto-plastic behavior of material under cyclic loading. Progression of plastic enclaves in the body shows the path of the plasticity. Strains, stresses, and displacements at any step of the analysis were evaluated. Weak-tension and equal tension and compression strength materials were used in this study.

From comparison of the results, it appears that, at least for the notched specimen, the plastic load carrying capacity of a material obeying a kinematic hardening rule is less than that of a material obeying an isotropic hardening rule for the Tresca yield surface. In general, using the method formulated herein leads to an analysis of the behavior of a ductile material under cyclic loading beyond the yield limit of the material.

Acknowledgment

The writers are grateful for partial support from National Science Foundation Grant PFR-8001506 and to Dr. Michael P. Gaus, program director. Special thanks to the Inelastic Behavior Committee of ASCE and to Joel I. Abrams for reviewing this paper and for their suggestions.

Appendix.—References

1. Allen, D. N. de G., and Southwell, R. V., "Relaxation Methods Applied to Engineering Problems—XIV: Plastic Straining in Two-Dimensional Stress Systems," *Philosophical Transactions, Royal Society of London*, Vol. 242, 1950, pp. 379–414.
2. Anand, S. C., Lee, S. L., and Rossow, E. C., "Finite Element Analysis of Elastic-Plastic Plane Stress Problems Based upon Tresca Yield Criterion," *Ingenieur-Archive*, Vol. 39, 1970, pp. 73–86.
3. Anand, S. C., and Weisgerber, F. E., "Inelastic Finite Element Analysis Using Tresca Yield Condition," *Journal of the Engineering Mechanics Division*, ASCE, Vol. 103, No. EM1, Feb., 1977, pp. 1–16.
4. Anand, S. C., and Weisgerber, F. E., "Usage of the Tresca Yield Condition in Finite Element Plane Strain Analysis," *International Journal of Solids and Structures*, Vol. 14, 1978, pp. 625–637.
5. Anand, S. C., "Constitutive Relations and Solution Schemes in Plastic Analysis," *Journal of the Engineering Mechanics Division*, ASCE, Vol. 106, No. EM1, Feb., 1980, pp. 21–36.
6. Armen, Jr., H., et al., "Plasticity," *Finite Element Techniques in Structural Mechanics*, H. Tottenham and C. Brebbia, eds., Southhampton University Press, 1970, pp. 209–257.
7. Armen, H., "Assumptions, Models, and Computational Methods for Plasticity," *Computer & Structures*, Vol. 10, 1979, pp. 161–174.
8. Gallagher, R. H., Padlog, J., and Bijlaard, P. P., "Stress Analysis of Heated Complex Shapes," *Journal of the American Rocket Society*, Vol. 32, 1962, pp. 700–707.
9. Koiter, W. T., "Stress-Strain Relations, Uniqueness and Variational Theorems for Elastic-Plastic Materials with Singular Yield Surface," *Quarterly of Applied Mathematics*, Vol. 11, 1953, pp. 350–354.
10. Lin, T. H., *Theory of Inelastic Structures*, John Wiley and Sons, Inc., New York, N.Y., 1968.
11. Marcal, P. V., and King, I. P., "Elasto-Plastic Analysis of Two-Dimensional Stress Systems by the Finite Element Method," *International Journal of Mechanical Science*, Vol. 9, 1967, pp. 143–155.
12. Massonnet, C., Olszak, W., and Phillips, A., *Plasticity in Structural Engineering Fundamentals and Applications*, Springer-Verlag, 1979.
13. Nayak, G. C., and Zienkiewiecz, "Elasto-Plastic Stress Analysis: A Generalization for Various Constitutive Relations Including Strain Softening," *International Journal for Numerical Methods in Engineering*, Vol. 5, 1972, pp. 113–135.
14. Pope, G. G., "A Discrete Element Method for the Analysis of Plane Elasto-Plastic Stress Problems," *The Aeronautical Quarterly*, Vol. XVII, Part 1, Feb., 1966, pp. 83–104.
15. Swedlow, T. L., Williams, M. L., and Yang, W. M., "Elasto-Plastic Stresses in Cracked Plates," *Report SM 65-19*, California Institute of Technology, 1965.
16. Theocaris, P. S., and Marketos, E., "Elastic-Plastic Strain and Stress Distribution in Notched Plates under Plane Stress," *Journal of the Mechanics and Physics of Solids*, Vol. 11, 1963, pp. 411–428.
17. Tillerson, J. R., Stricklin, J. A., and Haisler, W. E., "Numerical Methods for the Solution of Nonlinear Problems," *Numerical Solution of Nonlinear Structural Problems*, ASME, Nov., 1973, pp. 67–101.

18. Tocher, J. L., "Nonlinear Material Analysis with Finite Element and Incremental Methods," *Document No. D6-29460*, The Boeing Co., Commercial Airplane Division, Renton, Wash., 1968.
19. Torkamani, M. A. M., and Pajand, M. R., "Elastic-Plastic Analysis for Cyclic Loading and Tresca Yield Condition," *Research Report SETEC-CE-82-009*, Univ. of Pittsburgh, Dept. of Civ. Engrg., Pittsburgh, Pa., July, 1982.
20. Weisgerber, F. E., "Tresca Yield Condition in Elastic-Plastic Finite Element Analysis," thesis presented to Clemson University, in 1976, in partial fulfillment of the requirements for the degree of Doctor of Philosophy.
21. Yamada, Y., Yoshimura, N., and Sakurai, T., "Plastic Stress-Strain Matrix and its Application for the Solution of Elastic-Plastic Problems by the Finite Element Method," *International Journal of Mechanical Science*, Vol. 10, 1968, pp. 343–354.
22. Ziegler, H., "A Modification of Prager's Hardening Rule," *Quarterly of Applied Mathematics*, Vol. 17, No. 1, 1959, p. 55.
23. Zienkiewicz, O. C., Valliappan, S., and King, I. P., "Elasto-Plastic Solutions of Engineering Problems, Initial Stress, Finite Element Approach," *International Journal for Numerical Methods in Engineering*, Vol. 1, 1969, pp. 75–100.